Polymer Chemistry

ROYAL SOCIETY OF CHEMISTRY

PAPER

View Article Online
View Journal | View Issue

Cite this: *Polym. Chem.*, 2022, **13**, 2651

Catalyst-free transesterification vitrimers: activation *via* α-difluoroesters†

Florian Cuminet, [a,b] Dimitri Berne,[a] Sébastien Lemouzy,[a] Éric Dantras,[b] Christine Joly-Duhamel, [a] Sylvain Caillol, [a] Éric Leclerc[a] and Vincent Ladmiral *[a]

Received 28th January 2022,
Accepted 24th March 2022

DOI: 10.1039/d2py00124a

rsc.li/polymers

Transesterification vitrimers often require high catalyst loadings to achieve 3D networks reprocessable at moderately high temperature. The addition of an activating group close to the ester bonds allows to synthesize catalyst-free transesterification vitrimers. Here, we unveil the effect of the α-difluoromethylene group as a novel activating group for such materials. Fluorine features exceptional properties, in particular a strong electronegativity enabling CF_2 groups to activate the epoxy-acid polymerization, and more interestingly also the transesterification reaction on adjacent esters. Consequently, this fluorinated group affords the easy synthesis of a highly crosslinked reprocessable material that do not require any metallic or organic catalyst. This vitrimer is endowed with advantageous reprocessing abilities and underwent 10 consecutive cycles without loss of mechanical properties. In brief, the vitrimer combines durability, recyclability and is catalyst-free. This discovery is one step further towards recyclable greener polymers.

Introduction

For decades, polymer materials have been classified depending on their macromolecular structure. On the one hand are amorphous thermoplastics, composed of entangled linear chains. In these materials, polymer chains are not covalently bonded, and are able to slide on one another.[1] This translates, at the macroscopical scale, in their solubility in suitable solvents and in their ability to be reshaped upon heating. On the other hand are thermosets, composed of a 3D network. Theoretically, a thermoset is a single infinite macromolecule forming a covalently crosslinked network. This permanent structure leads to insolubility in solvents, and prevents recycling by simple thermal methods.[1,2] In the pursuit of greener, more sustainable polymers, thermosets remain a challenge for recycling.[3] Yet, they are assets in many applications for which thermal and chemical resistances are required. A third class of polymer materials consisting in a covalent crosslinked network in which the covalent bonds can be exchanged by reversible chemical reactions was proposed. They were called CANs, short for Covalent Adaptable Networks. In 2005, Bowman *et al.*[4] synthesized a covalently bonded 3D network alike thermosets, endowed with covalent bonds able to exchange *via* an associative mechanism upon irradiation with visible light. This concept was further developed by Leibler *et al.*[5] in 2011 with a material based on transesterification activated upon heating. This material was insoluble in common organic solvents even at high temperature, but able to flow and to be reshaped upon heating. Interestingly, this new kind of material exhibited an Arrhenian viscosity decrease with increasing temperature, a feature usually observed for inorganic glasses, or more generally for "strong" glasses in accordance with the work of Angell.[6] This analogy inspired the name vitrimers for such materials. Since this discovery, other kinds of exchangeable bonds such as carbonates,[7] boronic esters,[8,9] disulfides,[10,11] silyl ethers,[12,13] urethanes,[14–18] olefins,[19] imines,[20–23] vinylogous urethanes,[24–26] diketoenamines,[27] acylated acetals,[28,29] and trialkylsulfonium salts[30,31] have been investigated. Despite the success of vitrimers in materials research, they have yet to be implemented in industrial and commercial applications as they are not adapted to the recycling processes existing for thermoplastics.[32] Moreover, long reprocessing times at high temperatures can trigger premature degradation of the vitrimer after repeated reshaping processes.[33] To accelerate the reshaping process, one solution is the use of catalysts. However, some exchange reactions such as transesterification are so slow that they often require high loadings.[5] Yet, the use of catalysts raise concerns about the materials ageing or the risk of leaching,[34,35] which is

[a]*ICGM, Univ Montpellier, CNRS, ENSCM, Montpellier, France.*
E-mail: Vincent.ladmiral@enscm.fr
[b]*CIRIMAT, Université Toulouse 3 Paul Sabatier, Physique des Polymères, 118 Route de Narbonne, 31062 Toulouse, France*

†Electronic supplementary information (ESI) available: ^{1}H, ^{13}C, ^{19}F NMR spectra, FTIR spectra, TGA, DSC, DMA thermograms, EEW calculation details, gel time determination, gel content details and fitting parameters for stress relaxation experiments. See DOI: **https://doi.org/10.1039/d2py00124a**

undesirable for application such as food-contact materials for example. The first catalyst-free vitrimer was based on vinylogous urethanes exchange. This reaction is fast enough to afford short reprocessing times without catalyst.[25] Since this seminal article, other examples of catalyst-free vitrimers based on fast exchange reactions were proposed, such as hydroxyurethanes,[16] hemiacetal esters,[28] trialkylsulfonium salts,[31] oxime-esters[33] and imines.[36] Lowering the crosslinking density and increasing the number of exchangeable moieties were proven to enhance the reshaping abilities of catalyst-free materials.[37–41] However, since these parameters also influence the materials mechanical properties, this strategy may not be suitable to a wide range of applications. To overcome the risk of catalyst leaching, some vitrimers were also synthesized with a catalyst (amines for instance) embedded in the network.[42–44]

In 2015, Guan *et al.* proposed to implement in vitrimers the concept of neighboring group participation (NGP), well-known in the field of organic chemistry but new to the field of vitrimers.[45] Materials crosslinked using difunctional dioxaborolane and possessing neighboring amino groups relaxed faster than the one deprived of such groups. The potential of internal catalysis or internal activation and neighboring group participation (NGP) to tune CANs has recently been reviewed.[46,47] In their review, Van Lijsebetten *et al.*[46] made a clear distinction between NGP for which the neighboring group is involved with a covalent bond at some point of the reaction, and the broader concept of internal catalysis including effects such as inductive effects.

The present work focuses on transesterification vitrimers, as they usually require a catalyst. To address the concerns raised by the use of external catalysts, some functional groups were reported to be efficient for NGP, such as phthalate monoesters[48] or benzenesulfonic acid groups.[49] Such groups modify the transesterification mechanism and facilitate the exchange. Examples of activation by inductive effect were reported on Meldrum's acids in PDMS[50] or in polyimine vitrimers for instance.[51] In transesterification vitrimers, malonates were used to activate the exchange reaction.[52] Because of its high electronegativity, fluorine has a strong potential to activate bond exchanges. Indeed, the carbonyl group of fluorinated esters is known to be very electrophilic,[53] which facilitates hydrolysis and nucleophilic attack.[54,55] Fluorine substitution thus appear as a good strategy to activate transesterification reactions. Recently, a CF_3 group positionned on the α carbon of esters was demonstrated to have a significant activating effect on transesterification in polyester networks.[56] In the present work, fluorine atoms were added one atom closer to the ester bond and α-diflluoro esters are implemented for the first time to design a catalyst-free transesterification vitrimer. A trifunctional α-difluoro carboxylic acid was prepared and used in combination with a commercial diepoxide (butanediol diglycidyl ether, BDGE) to prepare an epoxy-acid network which displayed insolubility in organic solvents, but was able to be reshaped under relatively mild conditions without catalyst.

Results and discussion

α-Difluoro carboxylic acid monomer synthesis

Transesterification vitrimers require dangling hydroxy groups for the exchange reactions to happen. Fortunately, the epoxy opening by a carboxylic acid produces such groups in beta position to the ester. The strategy developed here therefore relies on the use of a trifunctional carboxylic acid monomer, and a commercial diepoxide to obtain a 3D network. To maximize the inductive effect of fluorine on the ester bond, the strongest fluorinated activating group (CF_2) should be positioned as close as possible to the exchangeable bond. A trifunctional monomer bearing three α-difluorocarboxylic acids was thus designed and synthesized in two steps from a commercial triphenol (1,1,1-tris(4-hydroxyphenyl)ethane, "TPE"). TPE was reacted with ethyl bromodifluoroacetate at 70 °C for 40 hours to obtain by nucleophilic substitution a mixture of the di- and trisubstituted esters (15 and 60 mol% respectively). After column chromatography, the resulting α-difluoro triester then underwent facile saponification to yield, after appropriate workup, the desired α-difluoro triacid (TPE-TAF) as a white waxy solid with an overall yield of 50% (Scheme 1).

Polymerization and curing

Butanediol diglycidyl ether (BDGE, ESI Fig. S14, S15 and sections A, B†) was identified as a promising commercial epoxy resin, as its viscosity is very low and because it can dissolve TPE-TAF before gelation happens. In addition, its structure advantageously adds flexibility to the network, may counterbalance the rigidity of the TPE-TAF structure, and might prevent a high T_g which would make the reprocessability of the material more difficult (Scheme 2).

TPE-TAF was dissolved in BDGE at room temperature (*ca.* 20 °C). The mixing time needed to be reduced to a few minutes only, to avoid the gelation caused by the fast reaction between the α-difluoro acids and the epoxides (even at room temperature) and ensure the homogeneity of the mixture. The mixture was then left at room temperature for at least 8 h, resulting into a brittle gel, which was then cured at 150 °C.

The gel time observed visually was consistent with the gel time determined by rheological analysis (Fig. S17†). At 20 °C, a gel time of 1.3 h was estimated at the crossover of loss and storage moduli, confirming that the epoxy opening by the α-difluoro carboxylic acid readily happens at room temperature. This behavior is highly unusual for epoxy-acid systems, which usually require catalysis and relatively high tempera-

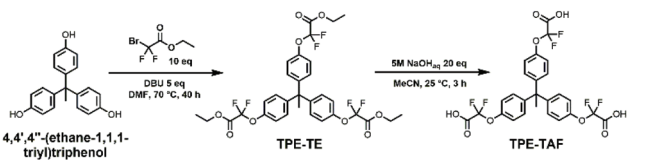

Scheme 1 2-Step synthesis of the trifunctional α-difluoro carboxylic acid TPE-TAF.

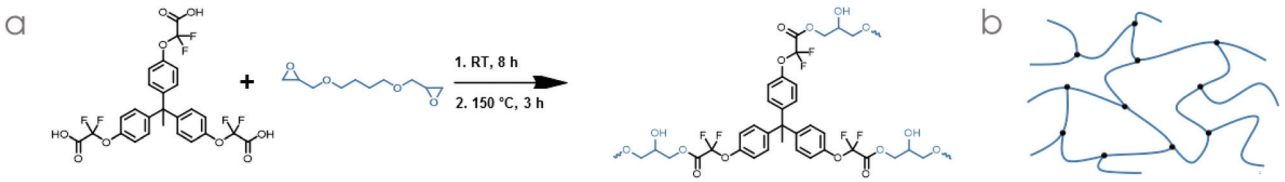

Scheme 2 (a) Network synthesis from TPE-TAF and BDGE and (b) schematic representation of the network.

tures (80–120 °C).[57] For catalyst-free systems, even higher temperatures (around 200 °C) are required.[58] This fast polymerization reaction at low temperature strongly suggests the activating inductive effect of fluorine atoms on the carboxylic acid towards the epoxy-opening reaction.

The polymerization kinetics at room temperature were monitored *via* FTIR. The disappearance of the epoxy band at 908 cm^{-1} was clearly observed but the conversion of acid functions at 1758 cm^{-1} into esters at 1761 cm^{-1} could not be determined, because the acid and ester bands overlapped too much (Fig. S22†). The epoxy band decreased significantly for the first 6 h of reaction, and then decreased at a much lower rate until the end of the acquisition after 64 h (Fig. 1). This rate change was probably due to the gelation of the mixture which slowed down the reaction between the remaining reactive species.

The material obtained after 4 days at room temperature was left for 3 h in an oven at 150 °C to ensure complete polymerization. Three consecutive DSC ramps were carried out on the resulting material. The thermograms overlaid perfectly, did not show any residual exotherm and revealed a T_g of 47 °C which did not evolve after any of these heating ramps (Fig. S18†). The curing of the material was thus deemed complete.

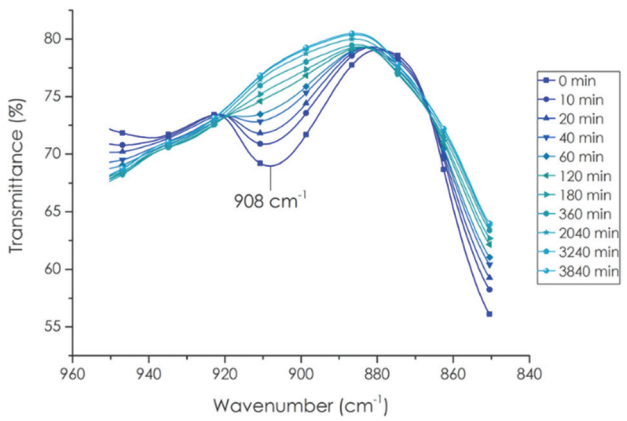

Fig. 1 Evolution of the epoxy FTIR band at 908 cm^{-1} of the TPE-TAF/BDGE binary mixture *versus* time at room temperature (*ca.* 20 °C).

Solubility tests were performed in acetone, THF, toluene, cyclohexane, DMSO, DCM and acetonitrile (Table S1†). The highest values were found for acetone and THF. In particular, after 24 h under agitation, an insoluble fraction of 94 ± 2% was measured in acetone (the best solvent for BDGE and TPE-TAF), thus proving that the curing process led to the formation of a 3D crosslinked material, as expected.

Vitrimer characterization

TGA under air showed that no significant mass loss was observed up to 200 °C, with a 2% and 5% degradation temperatures $T_{d2\%}$ and $T_{d5\%}$ of 205 °C and 262 °C respectively (Fig. S20† and Table 1). The T_g of the TPE-TAF/BDGE material was determined to be 47 °C (Fig. S18† and Table 1). TPE-TAF contains three aromatic cycles which bring rigidity to the polymer structure, whereas the linear structure of BDGE adds flexibility. This balance explains the moderate T_g value observed.

A few preliminary reshaping trials allowed to set the reshaping temperature value at 100 °C. The material stability to reprocessing cycles was then determined by isothermal TGA experiments performed at 100 °C for 16 h under air, to simulate the oxidative environment during reprocessing (Fig. 2 and Table 1). After 4 h, a mass loss of 4.3% was observed. The value stabilized to 4.4% after 5 h and did not evolve afterwards. This loss might be due to the evaporation of remaining traces of solvents trapped in the TPE-TAF after synthesis.

The kinetics of the flow behavior of the material was studied using stress-relaxation experiments. The relaxation modulus was monitored with time between 170 and 210 °C with 10 °C steps (Fig. 3). It is important to state here that analogous non fluorinated polyester epoxy network prepared using 0.1 mol% Zn catalyst by Leibler *et al.* did not show vitrimer properties.[5]

Normalized stress-relaxation experimental curves shown in Fig. 3 reveal that, in the 170 °C–210 °C temperature range, the TPE-TAF/BDGE network relaxed the stress applied. This behav-

Table 1 Table of the vitrimer properties

Gel content[a] (%)	$T_{d2\%}$ (°C)	Mass loss[b] (4 h, %)	Mass loss[b] (16 h, %)	T_g (°C)	T_α (°C)	E'_G[c] (GPa)	E'_R[d] (MPa)
94 ± 2	205	4.3	4.4	47	39	3.7	18.1

[a] Gel content in acetone at 20 °C for 24 h. [b] T = 100 °C. [c] Value at T_α −50 °C. [d] Value at T_α +50 °C.

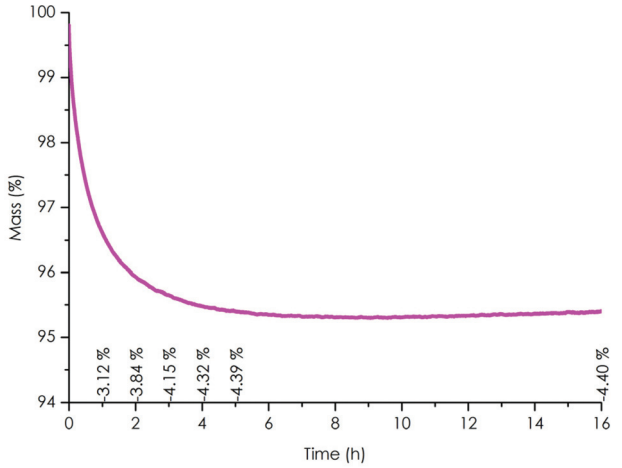

Fig. 2 Isothermal TGA thermogram of TPE-TAF/BDGE material under air at 100 °C (% mass loss).

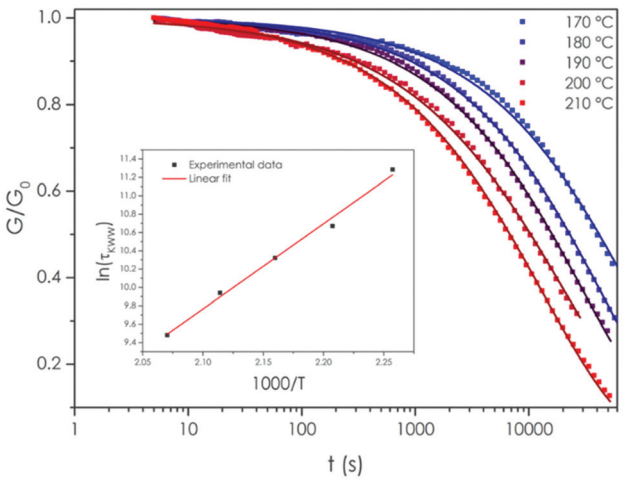

Fig. 3 Normalized stress–relaxation curves from 170 to 210 °C with 10 °C steps fitted with the Kohlrausch–Williams–Watts equation (KWW) and τ_{KWW} relaxation times reported in the Arrhenius diagram (inset, R^2 = 0.98985).

ior is expected only if the network is able to reorganise. The fact that this material flowed on the rubbery plateau proves that fluorine atoms activated the transesterification. A contribution from minute amounts of unreacted carboxylic acid function might as well favor the transesterification.[60] Furthermore, the relaxation rate depended on the temperature, as expected for a vitrimer.

The usual fitting model for such experiments is the exponential decay (Maxwell model). Nevertheless, this model did not fit well the experimental data obtained in the logarithmic time scale (R^2 between 0.934 and 0.989). A Kohlrausch–Williams–Watts "stretched exponential" equation was found to better fit (see Table S2† for the equation and the fitting parameters) the stress relaxation dataset[1] (R^2 between 0.995 and 0.99975, depending on the temperature). In KWW model, a stretch parameter β is added to the exponential decay. The closer to 1 is β, the closer to the Maxwell model are the data. From 170 °C to 210 °C, the value of β was about 0.56 ± 0.02, indicating that the flow kinetics was associated with a distribution of relaxations rather than with a single relaxation time kinetics.[1]

The relaxation time values obtained from the KWW fitting equations were plotted in an Arrhenius diagram (Fig. 3 inset) to determine the value of the flow activation energy E_a. This E_a was determined to be 77 kJ mol^{-1}, in good agreement with the 29–163 kJ mol^{-1} range reported so far for transesterification vitrimers,[47] especially for catalyst-free vitrimers activated by neighboring groups for which the activation energy values are ranging from 78 to 94 kJ mol^{-1}.[42,59–61]

The material relaxation observed in the absence of external catalyst demonstrated the activating effect on the transesterification of the two fluorine atoms located on the α-carbon of the esters , as non-catalyzed epoxy-acid networks usually exhibit no relaxation on a measurable time scale. As previously mentioned, tiny amounts of unreacted carboxylic acid, if present, could also add a contribution on this effect. A slight contribution from the phenoxy group is plausible, but would be much weaker than the contributions of the two fluorine atoms given the relative electronegativities of these elements (χ_F = 4.2, χ_O = 3.6). This is well illustrated by the pK_as of acetic acid 4.7, glycolic acid 3.8, phenoxyacetic acid 3.2 and difluoroacetic acid 1.2.[63,64] This range stresses out the difference in electron-withdrawing ability of two fluorine *vs.* one oxygen atom. The material behavior in temperature followed an Arrhenius law, as expected for a vitrimer. α-Difluoro esters are thus efficient activated esters for the design of catalyst-free transesterification vitrimers.

The discrepancy between the sluggishness in stress-relaxation experiments and the mild reprocessing conditions observed is striking. This difference can be explained by the pressure applied to the material,[65,66] which is an important and often overlooked parameter. The force applied onto the material during reprocessing is 8.8 times the force applied during relaxation experiments. The reprocessing experiments are thus carried out at high pressure value in compression, which explains the difference in the behavior observed.

Reprocessing classical thermosets by compression molding is impossible, in contrast to vitrimers which possess exchangeable bonds. The TPE-TAF/BDGE material was successfully reprocessed using compression-molding further demonstrating its vitrimer character. 1 mm^3 pieces of the material were reassembled into a small ribbon after 1.5 h at 100 °C under a 6 ton load. The required reprocessing conditions were relatively mild compared to transesterification vitrimers reported in literature, whether they are catalyzed or not (Fig. 4).[5,37,40,44,48,52,62,67–72]

Ten successive reprocessing cycles were successfully performed and each time homogeneous transparent samples were recovered. The color of the material did not significantly change with the successive reshaping cycles (Fig. 5). To quantitatively assess the material evolution with reprocessing, thermomechanical analyses were performed.

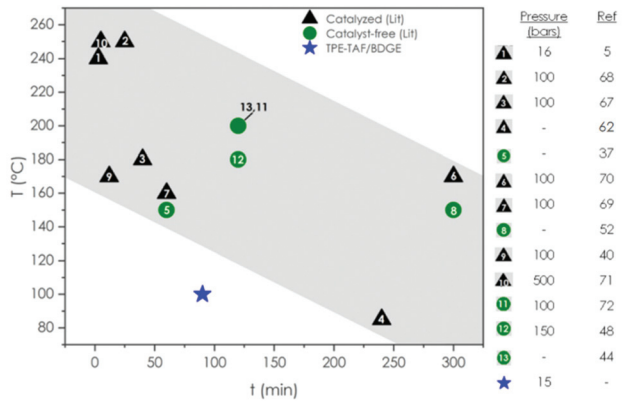

Fig. 4 Comparison of TPE-TAF/BDGE reprocessing temperature, pressure and time with various catalyzed and catalyst-free transesterification vitrimers reported so far.[5,37,40,44,48,52,62,67–72]

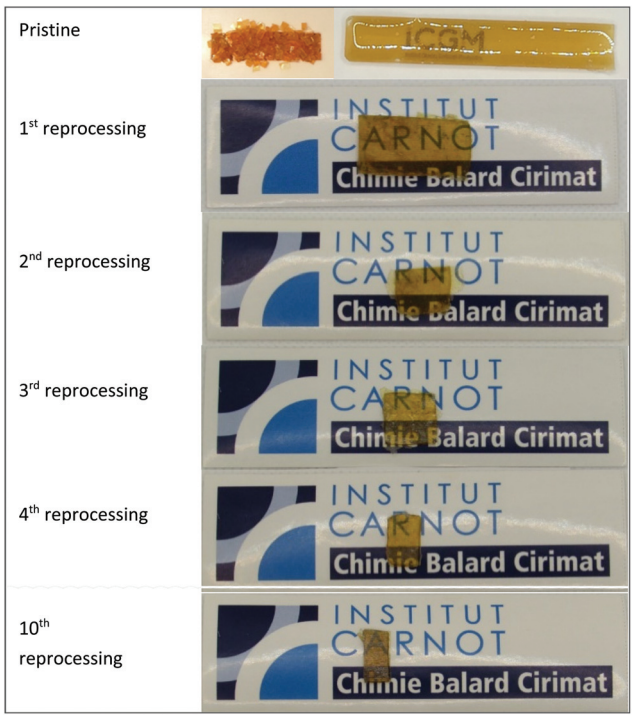

Fig. 5 TPE-TAF/BDGE aspect after several reprocessing cycles.

The TPE-TAF/BDGE material evolution with reprocessing was studied using DMA experiments. The values of the storage modulus E' in the glassy plateau and in the rubbery plateau regions, and the evolution of T_α allow to detect whether the TPE-TAF/BDGE material mechanical properties decrease after several reprocessing cycles. A ramp from −100 to +150 °C was performed after each reprocessing cycle to check whether the mechanical properties were fully recovered.

The pristine material exhibited a glassy plateau storage modulus E'_G = 3.7 GPa, a rubbery plateau storage modulus E'_R = 18 MPa and a T_α = 39 °C, which is consistent with the values reported in the literature[37,70,72–74] for epoxy-acid and epoxy-anhydride vitrimers (Table 2 and Fig. S19†).

Table 2 Evolution of DMA characteristic values before and after 10 reprocessing cycles

Reprocessing cycle	T_α (°C)	E'_G [a] (GPa)	E'_R [b] (MPa)
Pristine	39	3.7	18.1
10	49	3.9	18.7

[a] Value at T_α −50 °C. [b] Value at T_α +50 °C.

Table 3 Evolution of T_α with the successive reprocessing cycles

Reprocessing cycle	Pristine	1	2	3–10
T_α (°C)	39	41	47	49

Upon the first three reprocessing cycles, the T_α increased from 39 °C to 41, 47 and 49 °C respectively, suggesting that the crosslink density slightly increased after each reshaping step, which is consistent with the increase of the rubbery plateau modulus (Table 2). After this 3rd reshaping process, the T_α value did not change with further reprocessing cycles up to the tenth cycle (Table 3).

The storage modulus (E') value in the glassy plateau region slightly changed from 3.7 to 3.9 GPa for the pristine network and after the tenth reprocessing respectively. Similarly, the value of E' in the rubbery plateau region increased by a mere 0.6 MPa (Table 2) (from 18.1 to 18.7 MPa for the pristine and 10th reprocessing cycle). These results show that there is no significant evolution of the network after 10 cycles.

Conclusion

In summary, polyester vitrimers were prepared out of a synthesized trifunctional α-difluoroacid and a commercially available difunctional epoxy resin. Thanks to the activation of the acid by the fluorine atoms, the epoxy-acid polymerization reaction happened readily at room temperature, whereas catalysts and high temperatures are usually needed for non-fluorinated systems. The resulting TPE-TAF/BDGE material was insoluble yet able to be reprocessed under mild conditions (100 °C, 1.5 h, 6 t). As expected, α-difluoro ester underwent significantly accelerated transesterification. This activation was such that no external catalyst was needed, in contrast to most other transesterification vitrimers. The flow activation energy E_a was evaluated to be 77 kJ mol^{-1} which is consistent with the values reported for transesterification vitrimers catalysed by internal amines for instance, but also very close to the value (67–72 kJ mol^{-1}) obtained for α-CF_3 activation.[56] This polymer proved highly stable over repeated reprocessing cycles, with very little degradation of the mechanical properties observed after 10 cycles. The proof-of-concept based on the high electron withdrawing effect of fluorinated groups and exposed here is very

promising to tune vitrimers properties and address the concerns related to the use of external catalysts, such as premature ageing, leaching of the catalyst or limited reprocessing abilities.[34,35,75]

Experimental section

Materials

1,4-Butanediol diglycidyl ether (BDGE, Aldrich, ≥95%, NMR spectra, FTIR spectrum and EEW calculations in ESI Fig. S14, S15† and sections A, B), 1,1,1-Tris(4-hydroxyphenyl)ethane ("TPE", Sigma-Aldrich, 99%), 1,8-Diazabicyclo(5.4.0)undec-7-ene (DBU, Fluorochem, 98%), ethyl bromodifluoroacetate (Fluorochem, 98%), benzophenone (Avocado Research Chemicals Ltd, 99%), succinic acid (ABCR, 99%) were used as received. Solvents were supplied by VWR Chemicals. Deuterated solvents were supplied by Eurisotop (99.8%).

Synthetic procedures

"TPE-TE" compound. 1,1,1-Tris(4-hydroxyphenyl) ethane (6.13 g, 20 mmol, 1 equiv.) was dissolved in dry DMF (120 mL, 0.16 M). 1,8-Diazabicyclo [5.4.0] undec-7-ene (DBU, 15 mL, 100 mmol, 5 equiv.) was added in one portion and the reaction was heated to 70 °C. Ethyl bromodifluoroacetate (12.8 mL, 100 mmol, 5 equiv.) was then added *via* a syringe pump at a rate of 5.0 mL h^{-1} and the reaction was stirred at 70 °C for 40 h. The resulting reaction mixture was very dark due to the probable oxidation of some of the phenol reagents, which could not be prevented even under argon atmosphere or protection from light. The crude mixture was cooled to room temperature, diluted with H_2O (600 mL), and extracted 5 times with Et_2O (5 × 100 mL). The combined organic layers were washed with 2 × 150 mL water and with 150 mL of brine, dried with Na_2SO_4, filtered, and concentrated under reduced pressure. The dark-brown crude mixture was purified by column chromatography on silica gel using pentane/ethyl acetate mixtures (5/1, 3/1 and finally 1/1) as eluent to afford the pure triester (F1: 8.2 g, 61%, white solid) and diester (F2: 1.8 g, 16%, off-yellow viscous oil).

Triester TPE-TE characterizations (NMR spectra in Fig. S1 to S3†): **^{1}H NMR 400MHz $CDCl_3$:** δ 7.15–7.10 (m, 6H, aromatic protons, *m*-OCF_2), 7.07–7.02 (m, 6H, aromatic protons, *o*-OCF_2), 4.39 (q, ^3J = 7.2 Hz, 6H, OCH_2CH_3), 2.15 (s, 3H, Ar_3C-CH_3), 1.36 (t, ^3J = 7.1 Hz, 9H, OCH_2CH_3). **^{19}F NMR 377 MHz, $CDCl_3$:** δ −76.41. **^{13}C NMR 101 MHz, $CDCl_3$:** δ 159.9 (CO_2Et, t, $^2J_{C-F}$ = 41.5 Hz), 148.0 (*ipso*-^{Ar}C-O, t, $^3J_{C-F}$ = 2.0 Hz), 146.5 (*ortho*-^{Ar}C-O, t, $^4J_{C-F}$ = 2.0 Hz), 129.9 (*ipso*-^{Ar}C-C-CH_3), 121.2 (*ortho*-^{Ar}C-C-CH_3), 114.1 (OCF_2, t, $^1J_{C-F}$ = 272.5 Hz), 63.8 (O-CH_2CH_3), 51.7 (Ar-C-CH_3), 30.9 (Ar-C-CH_3), 14.0 (O-CH_2CH_3). R_f (petroleum ether : ethyl acetate 5 : 1) = 0.42. **HRMS (ESI+)** Calc. for $[M + Na]^+$ 695.1686, found 695.1677.

Disubstituted ester characterizations (NMR spectra Fig. S4 to S8†): **^{1}H NMR 400MHz $CDCl_3$:** δ 7.14–7.08 (m, 4H, aromatic protons, *m*-OCF_2), 7.07–7.03 (m, 4H aromatic protons, *o*-OCF_2), 6.95–6.89 (m, 2H aromatic protons, *m*-OH), 6.79–6.72 (m, 2H, aromatic protons, *o*-OH), 5.06 (s, 1H, O*H*), 4.39 (q, ^3J = 7.1 Hz, 4H, OCH_2CH_3), 2.12 (s, 3H, Ar_3C-CH_3), 1.36 (t, ^3J = 7.2 Hz, 6H, OCH_2CH_3). **^{19}F NMR 377 MHz, $CDCl_3$:** δ −76.34. **^{13}C NMR 101 MHz, $CDCl_3$:** δ 160.0 (CO_2Et, t, $^2J_{C-F}$ = 41.2 Hz), 154.1, 147.7 (*ipso*-^{Ar}C-O, t, $^3J_{C-F}$ = 2.0 Hz), 147.2, 140.6, 129.9, 129.9, 121.1 (*ortho*-^{Ar}C-O t, $^4J_{C-F}$ = 0.7 Hz), 115.0, 114.1 (OCF_2, t, $^1J_{C-F}$ = 272.4 Hz), 63.8 (O-CH_2CH_3), 51.4 (Ar-C-CH_3), 30.9 (Ar-C-CH_3), 14.0 (O-CH_2CH_3). R_f (petroleum ether : ethyl acetate 5 : 1) = 0.30.

"TPE-TAF" compound. In a 250 mL round bottom flask, 7 g of triester were dissolved in acetonitrile (90 mL). Then, a 5 M aqueous solution of NaOH (12.5 g in 62 mL) was added slowly at room temperature, and the mixture was stirred for 3 h. 200 mL of a saturated $NaHCO_3$ solution was added to the mixture and the aqueous layer was washed with 100 mL of diethyl ether. The organic layer was extracted with 50 mL of saturated $NaHCO_3$ solution, and the gathered aqueous layers were acidified to pH = 1 using 2 M HCl. Finally, the acidified aqueous layer was extracted with 3 × 100 ml of diethyl ether, and the solvent was removed under high vacuum to afford the desired triacid as a white waxy solid (yield over the two steps η = 50%, purity >98% estimated from ^{1}H NMR spectrum). Up to 9 grams per batch could be obtained.

Trifunctional acid TPE-TAF characterizations (NMR spectra, FTIR spectrum and TGA thermogram in Fig. S9 to S13†): **^{1}H NMR 400MHz d_6-acetone:** δ 7.89 (br s, 3H, COO*H*), 7.20 (m, 12H, aromatic protons), 2.22 (s, 3H, C-CH_3). **^{19}F NMR 377 MHz, d_6-acetone:** δ −77.50. **^{13}C NMR 101 MHz, d_6-acetone:** δ 160.9 (COOH, t, $^2J_{C-F}$ = 40.7 Hz), 148.9 (*ipso*-^{Ar}C-O, t, $^3J_{C-F}$ = 2.0 Hz), 147.6, 130.8, 121.8, 115.3 (OCF_2, t, $^1J_{C-F}$ = 270.9 Hz), 52.4 (C-CH_3), 30.9 (C-CH_3). **HRMS (ESI+)** Calc. for $[M + Na]^+$ 611.0747, found 611.0750.

Determination of the epoxy equivalent weight (EEW)

The EEW of the BDGE was evaluated by NMR titration using benzophenone as standard in deuterated chloroform (experimental details are given in ESI section A†). This value was confirmed by DSC studies using succinic acid as the curing agent (experimental details are given in ESI section B†). The procedure was described in a previous article.[76] Several BDGE/succinic acid ratios were used to make a series of thermosets. The highest T_g was achieved for a 1 : 1 stoichiometry, from which the EEW was calculated.

"TPE-TAF/BDGE" vitrimer

Typically, 1.156 g (5.90 meq COOH) of TPE-TAF was quickly mixed manually in a 10 mL beaker with 0.682 g (5.93 meq epoxy) of BDGE at room temperature (*ca.* 20 °C) until the acid was fully dissolved. A clear yellowish viscous liquid was obtained and quickly cast in PTFE molds. The mixture was left at least 8 h at room temperature for gelation. The resulting material (TPE-TAF/BDGE) was then removed from the molds and cured 3 h at 150 °C.

Instrumentation

NMR. ^{1}H, ^{13}C and ^{19}F were acquired on a Bruker Avance 400 MHz spectrometer at 23 °C. External reference was tetramethylsilane (TMS) with chemical shifts given in ppm. Samples were diluted in 0.5 mL of $CDCl_3$ or DMSO-d_6 depending on their solubility.

FTIR. FTIR spectra and single wavenumber measurements were acquired on a ThermoScientific Nicolet iS50 FT-IR equipped with an attenuated total reflectance cell (ATR). The data were analyzed using the software OMNIC Series 8.2 from Thermo Scientific.

Mechanical characterizations. Gel time experiment was performed at 1 Hz with a 20 mm plane-plane geometry on a ThermoScientific Haake Mars 60 rheometer equipped with a Peltier heating cell. A 30 mL h^{-1} nitrogen flux was applied. Stress relaxation experiments were performed on the same apparatus equipped with a textured 8 mm plane-plane geometry. A 10% torsional strain was applied on 8 mm diameter and 2 mm thickness circular samples, and the rubbery modulus evolution with time was monitored.

DMA. Dynamic Mechanical Analyses were carried out on Metravib DMA 25 with Dynatest 6.8 software. Uniaxial stretching of samples ($1 \times 5 \times 12$ mm^3) was performed while heating at a rate of 3 °C min^{-1} from −90 °C to 150 °C, keeping the frequency at 1 Hz.

TGA. Thermogravimetric thermograms were recorded on a TA TGA G50 instrument using a 40 mL min^{-1} flux of synthetic air as purge gas. Approximately 10 mg of sample were used for each analysis. Ramps from 20 to 500 °C were applied at a rate of 20 °C min^{-1}.

DSC. Analyses were carried out using a NETZSCH DSC200F3 calorimeter. The calibration was performed using adamantane, biphenyl, indium, tin, bismuth and zinc standards. Nitrogen was used as purge gas. Approximately 10 mg of sample were placed in perforated aluminum pans and the thermal properties were recorded between −100 °C and the temperature of 2% degradation $T_{d2\%}$ at 20 °C min^{-1}. The reported values are the values measured during the second heating ramp.

Reprocessing. the material was cut into $1 \times 1 \times 1$ mm^3 pieces and then pressed in a PTFE mold for 1.5 h at 100 °C under a 6 tons load using a Carver 3960 manual heating press.

Author contributions

Conceptualization: FC, SC, ED, SL, EL, VL. Funding acquisition: SC, ED, EL, VL. Investigation: FC, SL. Methodology: all authors. Project administration: SC, ED, EL, VL. Supervision: FC, SC, ED, EL, VL. Validation: all authors. Visualization: FC. Writing – original draft: FC. Writing – review & editing: all authors.

Conflicts of interest

There are no conflicts to declare.

Acknowledgements

This work was funded by the Institut Carnot Chimie Balard CIRIMAT (16CARN000801) and the French National Research Agency ANR (AFCAN project – ANR-19-CE06-0014). The authors would like to thank Lise Reymond for her contribution to TPE-TAF synthesis, as well as Dr Marc Guerre and Dr François Tournilhac for fruitful discussions.

Notes and references

1 G. M. Scheutz, J. J. Lessard, M. B. Sims and B. S. Sumerlin, *J. Am. Chem. Soc.*, 2019, **141**, 16181–16196.
2 J.-P. Pascault, H. Sautereau, J. Verdu and R. J. J. Williams, *Thermosetting Polymers*, Marcel Dekker, Inc., New York, 2002.
3 S. J. Pickering, in *Wiley Encyclopedia of Composites*, John Wiley & Sons, Inc., Hoboken, New Jersey, 2012.
4 T. F. Scott, A. D. Schneider, W. D. Cook and C. N. Bowman, *Science*, 2005, **308**, 1615–1617.
5 D. Montarnal, M. Capelot, F. Tournilhac and L. Leibler, *Science*, 2011, **334**, 965–968.
6 C. A. Angell, *J. Non-Cryst. Solids*, 1991, **131–133**, 13–31.
7 R. L. Snyder, D. J. Fortman, G. X. De Hoe, M. A. Hillmyer and W. R. Dichtel, *Macromolecules*, 2018, **51**, 389–397.
8 M. Röttger, T. Domenech, R. Van Der Weegen, A. Breuillac, R. Nicolaÿ and L. Leibler, *Science*, 2017, **356**, 62–65.
9 F. Caffy and R. Nicolaÿ, *Polym. Chem.*, 2019, **10**, 3107–3115.
10 A. Ruiz de Luzuriaga, R. Martin, N. Markaide, A. Rekondo, G. Cabañero, J. Rodríguez and I. Odriozola, *Mater. Horiz.*, 2016, **3**, 241–247.
11 Z. Ma, Y. Wang, J. Zhu, J. Yu and Z. Hu, *J. Polym. Sci., Part A: Polym. Chem.*, 2017, **55**, 1790–1799.
12 Y. Nishimura, J. Chung, H. Muradyan and Z. Guan, *J. Am. Chem. Soc.*, 2017, **139**, 14881–14884.
13 X. Wu, X. Yang, R. Yu, X. J. Zhao, Y. Zhang and W. Huang, *J. Mater. Chem. A*, 2018, **6**, 10184–10188.
14 N. Zheng, Z. Fang, W. Zou, Q. Zhao and T. Xie, *Angew. Chem., Int. Ed.*, 2016, **55**, 11421–11425.
15 N. Zheng, J. Hou, Y. Xu, Z. Fang, W. Zou, Q. Zhao and T. Xie, *ACS Macro Lett.*, 2017, **6**, 326–330.
16 D. J. Fortman, J. P. Brutman, C. J. Cramer, M. A. Hillmyer and W. R. Dichtel, *J. Am. Chem. Soc.*, 2015, **137**, 14019–14022.
17 D. J. Fortman, J. P. Brutman, M. A. Hillmyer and W. R. Dichtel, *J. Appl. Polym. Sci.*, 2017, **134**, 44984.
18 X. Chen, L. Li, K. Jin and J. M. Torkelson, *Polym. Chem.*, 2017, **8**, 6349–6355.
19 Y.-X. Lu and Z. Guan, *J. Am. Chem. Soc.*, 2012, **134**, 14226–14231.
20 H. Zhang, D. Wang, W. Liu, P. Li, J. Liu, C. Liu, J. Zhang, N. Zhao and J. Xu, *J. Polym. Sci., Part A: Polym. Chem.*, 2017, **55**, 2011–2018.
21 S. Wang, S. Ma, Q. Li, X. Xu, B. Wang, K. Huang, Y. Liu and J. Zhu, *Macromolecules*, 2020, **53**, 2919–2931.
22 H. Zheng, Q. Liu, X. Lei, Y. Chen, B. Zhang and Q. Zhang, *J. Mater. Sci.*, 2019, **54**, 2690–2698.

23 R. Hajj, A. Duval, S. Dhers and L. Avérous, *Macromolecules*, 2020, **53**, 3796–3805.
24 W. Denissen, M. Droesbeke, R. Nicolaÿ, L. Leibler, J. M. Winne and F. E. Du Prez, *Nat. Commun.*, 2017, **8**, 14857.
25 W. Denissen, G. Rivero, R. Nicolaÿ, L. Leibler, J. M. Winne and F. E. Du Prez, *Adv. Funct. Mater.*, 2015, **25**, 2451–2457.
26 M. Guerre, C. Taplan, R. Nicolaÿ, J. M. Winne and F. E. Du Prez, *J. Am. Chem. Soc.*, 2018, **140**, 13272–13284.
27 P. R. Christensen, A. M. Scheuermann, K. E. Loeffler and B. A. Helms, *Nat. Chem.*, 2019, **11**, 442–448.
28 D. Boucher, J. Madsen, N. Caussé, N. Pébère, V. Ladmiral and C. Negrell, *Reactions*, 2020, **1**, 89–101.
29 D. Boucher, J. Madsen, L. Yu, Q. Huang, N. Caussé, N. Pébère, V. Ladmiral and C. Negrell, *Macromolecules*, 2021, **54**, 6772–6779.
30 Z. Tang, Y. Liu, Q. Huang, J. Zhao, B. Guo and L. Zhang, *Green Chem.*, 2018, **20**, 5454–5458.
31 B. Hendriks, J. Waelkens, J. M. Winne and F. E. Du Prez, *ACS Macro Lett.*, 2017, **6**, 930–934.
32 W. Alabiso and S. Schlögl, *Polymers*, 2020, **12**, 1660.
33 C. He, S. Shi, D. Wang, B. A. Helms and T. P. Russell, *J. Am. Chem. Soc.*, 2019, **141**, 13753–13757.
34 J. Wang, S. Chen, T. Lin, J. Ke, T. Chen, X. Wu and C. Lin, *RSC Adv.*, 2020, **10**, 39271–39276.
35 J. J. Lessard, L. F. Garcia, C. P. Easterling, M. B. Sims, K. C. Bentz, S. Arencibia, D. A. Savin and B. S. Sumerlin, *Macromolecules*, 2019, **52**, 2105–2111.
36 S. Dhers, G. Vantomme and L. Avérous, *Green Chem.*, 2019, **21**, 1596–1601.
37 J. Han, T. Liu, C. Hao, S. Zhang, B. Guo and J. Zhang, *Macromolecules*, 2018, **51**, 6789–6799.
38 F. I. Altuna, V. Pettarin and R. J. J. Williams, *Green Chem.*, 2013, **15**, 3360–3366.
39 C. Hao, T. Liu, S. Zhang, L. Brown, R. Li, J. Xin, T. Zhong, L. Jiang and J. Zhang, *ChemSusChem*, 2019, **12**, 1049–1058.
40 S. Mu, Y. Zhang, J. Zhou, B. Wang and Z. Wang, *ACS Sustainable Chem. Eng.*, 2020, **8**, 5296–5304.
41 T. Liu, B. Zhao and J. Zhang, *Polymer*, 2020, **194**, 122392.
42 F. I. Altuna, C. E. Hoppe and R. J. J. Williams, *Eur. Polym. J.*, 2019, **113**, 297–304.
43 C. Hao, T. Liu, S. Zhang, W. Liu, Y. Shan and J. Zhang, *Macromolecules*, 2020, **53**, 3110–3118.
44 Y. Li, T. Liu, S. Zhang, L. Shao, M. Fei, H. Yu and J. Zhang, *Green Chem.*, 2020, **22**, 870–881.
45 O. R. Cromwell, J. Chung and Z. Guan, *J. Am. Chem. Soc.*, 2015, **137**, 6492–6495.
46 F. Van Lijsebetten, J. O. Holloway, J. M. Winne and F. E. Du Prez, *Chem. Soc. Rev.*, 2020, **49**, 8425–8438.
47 F. Cuminet, S. Caillol, E. Dantras, E. Leclerc and V. Ladmiral, *Macromolecules*, 2021, **54**, 3927–3961.
48 S. Wang, N. Teng, J. Dai, J. Liu, L. Cao, W. Zhao and X. Liu, *Polymer*, 2020, **210**, 123004.
49 H. Zhang, S. Majumdar, R. A. T. M. Van Benthem, R. P. Sijbesma and J. P. A. Heuts, *ACS Macro Lett.*, 2020, **9**, 272–277.
50 B. M. El-Zaatari, J. S. A. Ishibashi and J. A. Kalow, *Polym. Chem.*, 2020, **8**, 1–3.
51 S. K. Schoustra, J. A. Dijksman, H. Zuilhof and M. M. J. Smulders, *Chem. Sci.*, 2021, **12**, 293–302.
52 S. Debnath, S. Kaushal and U. Ojha, *ACS Appl. Polym. Mater.*, 2020, **2**, 1006–1013.
53 P. G. Blake and B. F. Shraydeh, *Int. J. Chem. Kinet.*, 1981, **13**, 463–471.
54 G. Schmeer and P. Sturm, *Phys. Chem. Chem. Phys.*, 1999, **1**, 1025–1030.
55 J.-P. Brégué and D. Bonnet-Delpont, in *Bioorganic and Medicinal Chemistry of Fluorine*, John Wiley & Sons Inc., Hoboken, 2008.
56 D. Berne, F. Cuminet, S. Lemouzy, C. Joly-Duhamel, R. Poli, S. Caillol, E. Leclerc and V. Ladmiral, *Macromolecules*, 2022, acs.macromol.1c02538.
57 P.-J. Madec and E. Maréchal, *Adv. Polym. Sci.*, 1985, **71**, 153–228.
58 L. Shechter, J. Wynstra and R. P. Kurkjy, *Ind. Eng. Chem.*, 1957, **49**, 1107–1109.
59 M. Hayashi, *ACS Appl. Polym. Mater.*, 2020, **2**, 5365–5370.
60 A. Adjaoud, A. Trejo-Machin, L. Puchot and P. Verge, *Polym. Chem.*, 2021, **12**, 3276–3289.
61 T. Liu, C. Hao, L. Shao, W. Kuang, L. Cosimbescu, K. L. Simmons and J. Zhang, *Macromol. Rapid Commun.*, 2020, 2000458.
62 J. L. Self, N. D. Dolinski, M. S. Zayas, J. R. de Alaniz and C. M. Bates, *ACS Macro Lett.*, 2018, **7**, 817–821.
63 K. U. Goss, *Environ. Sci. Technol.*, 2008, **42**, 456–458.
64 N. V. Hayes and G. E. K. Branch, *J. Am. Chem. Soc.*, 1943, **65**, 1555–1564.
65 A. M. Hubbard, Y. Ren, D. Konkolewicz, A. Sarvestani, C. R. Picu, G. S. Kedziora, A. Roy, V. Varshney and D. Nepal, *ACS Appl. Polym. Mater.*, 2021, **3**, 1756–1766.
66 H. Fang, W. Ye, Y. Ding and H. H. Winter, *Macromolecules*, 2020, **53**, 4855–4862.
67 H. Zhang, C. Cai, W. Liu, D. Li, J. Zhang, N. Zhao and J. Xu, *Sci. Rep.*, 2017, **7**, 11833.
68 Y. Zhou, J. G. P. Goossens, R. P. Sijbesma and J. P. A. Heuts, *Macromolecules*, 2017, **50**, 6742–6751.
69 X. Yang, L. Guo, X. Xu, S. Shang and H. Liu, *Mater. Des.*, 2020, **186**, 108248.
70 T. Liu, S. Zhang, C. Hao, C. Verdi, W. Liu, H. Liu and J. Zhang, *Macromol. Rapid Commun.*, 2019, **40**, 1800889.
71 M. Giebler, C. Sperling, S. Kaiser, I. Duretek and S. Schlögl, *Polymers*, 2020, **12**, 1148.
72 Y. Liu, S. Ma, Q. Li, S. Wang, K. Huang, X. Xu, B. Wang and J. Zhu, *Eur. Polym. J.*, 2020, **135**, 109881.
73 F. I. Altuna, C. E. Hoppe and R. J. J. Williams, *Eur. Polym. J.*, 2019, **113**, 297–304.
74 J. Han, T. Liu, S. Zhang, C. Hao, J. Xin, B. Guo and J. Zhang, *Ind. Eng. Chem. Res.*, 2019, **58**, 6466–6475.
75 W. Denissen, J. M. Winne and F. E. Du Prez, *Chem. Sci.*, 2016, **7**, 30–38.
76 F. Jaillet, M. Desroches, R. Auvergne, B. Boutevin and S. Caillol, *Eur. J. Lipid Sci. Technol.*, 2013, **115**, 698–708.

